

激光—等离子弧复合焊温度场的数值模拟

李志宁, 常保华, 都东, 王力

(清华大学 先进成形制造教育部重点实验室, 北京 100084)

摘要: 利用峰值热流随深度衰减的高斯体热源与高斯面热源相结合的方法, 建立了激光—等离子弧复合焊三维运动热源模型, 重点考虑了由热源间距引起的激光束与等离子弧之间相互作用对热源模型的影响。基于所建立的热源模型对 2 mm 厚 1420 铝锂合金板的激光—等离子弧复合焊接温度场进行了有限元分析, 得到了不同热源间距条件下焊接区域的温度场分布。结果表明, 仿真结果与试验结果相符合, 证明了该热源模型是反映了客观实际的。此工作对于激光—电弧复合焊接传热及工艺研究具有指导意义。

关键词: 激光—等离子弧复合焊接; 有限元; 数值模拟; 铝锂合金

中图分类号: TG456.7 文献标识码: A 文章编号: 0253-360X(2007)06-029-05



李志宁

0 序 言

采用能量密度高、指向性好的等离子弧作为第二热源与激光复合可以实现薄板的高速、精密焊接^[1,2]。研究表明, 热源间距是影响复合焊焊缝成形的主要因素之一^[3]。研究复合焊的传热过程可以更好地理解热源间距对成形的影响规律, 但激光束与电弧之间存在复杂的相互作用, 采用数值仿真技术结合, 试验验证是一种较好的研究方法。目前, 国内外激光—电弧复合焊接的传热数值仿真研究还十分有限。文献[4]研究了激光—MIG 的传热、传质过程, 考虑了小孔中等离子体对激光的吸收作用。文献[5]建立了激光—TIG 的热源模型, 激光热源采用了点、线组合热源, TIG 采用面热源, 利用沿厚度方向的衰减系数来考虑小孔效应及激光与等离子体之间的相互作用。文献[6]利用旋转高斯体热源结合高斯面热源建立了激光—TIG 的热源模型, 但是选取激光与电弧间相互作用的修正系数则缺乏试验数据和理论支持。文献[7]采用高斯体热源结合面热源的方法建立了激光—TIG 复合焊接不锈钢的热源模型, 对于激光与电弧的相互作用, 主要依经验来修正。除了文献[4]的模型采用了自主开发的 FDM 程序计算外, 文献[5-7]的模型均利用商用 FEM 软件平台计算并得到了固定激光功率、不同电弧电流情况下的焊缝熔宽, 但在上述文献的模型中均没有考

虑不同热源间距对熔宽的影响。

在以上研究工作的基础上, 首先建立了激光—等离子弧复合焊三维热源运动模型, 在模型中考虑了不同热源间距条件下激光与电弧等离子体之间的相互作用, 然后通过不同热源间距条件下的 1420 铝锂合金复合焊接工艺试验来验证计算模型的正确性。

1 复合焊接热源模型的建立

1.1 激光—等离子弧的运动热源模型

考虑到焊接中激光的穿透作用, 可采用峰值热流沿深度衰减的高斯体热源模型^[8], 即

$$Q(r_1, z) = \frac{6P_{\text{laser}}(z+h)}{\pi h^2 R_{\text{laser}}^2} \exp\left(-\frac{3r_1^2}{R_{\text{laser}}^2}\right), \quad (1)$$

式中: P_{laser} 为有效的激光焊接功率; R_{laser} 为激光热流的作用半径; h 为热流作用深度; z 为工件沿 z 方向坐标; $r_1 = \sqrt{(x-x_{10})^2 + (y-y_{10})^2}$, x_{10} , y_{10} 为体热源中心坐标。

由于等离子弧热源功率较小, 没有穿透作用, 假定其符合高斯面热源, 可表示为

$$Q(r_2) = \frac{3\eta_{\text{arc}}UI}{\pi R_{\text{arc}}^2} \exp\left(-\frac{3r_2^2}{R_{\text{arc}}^2}\right), \quad (2)$$

式中: U 为电弧电压; I 为焊接电流; η_{arc} 为等离子弧的热效率; R_{arc} 为等离子弧热流的作用半径; $r_2 = \sqrt{(x-x_{a0})^2 + (y-y_{a0})^2}$, x_{a0} , y_{a0} 是面热源中心坐标。

收稿日期: 2006-07-10

基金项目: 高等学校博士学科专项科研基金(20050003041); 国防科技重点实验室基金(514610105005JW120)

运动的复合热源如图1所示, x, y, z 为坐标轴, v 为焊接速度, d 为激光与等离子弧热源中心距离。显然, $y_{t0} = vt, y_{a0} = y_{t0} + d, x_{t0} = x_{a0}, t$ 为焊接时间。

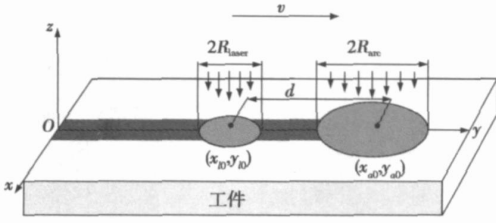


图1 复合热源运动示意图

Fig. 1 Moving heat source of hybrid welding

1.2 激光与电弧等离子体间相互作用的模型

在复合焊接过程中, 激光、等离子弧热源间距比较小时, 电弧的高温等离子体会对激光产生折射和吸收。根据文献[9], 吸收系数 α 主要由电弧空间的电子密度 N_e 、离子密度 N_i 和温度 T 确定, 但电子、离子密度和温度难以精确测量, 无法直接计算电弧对激光的吸收系数。根据文献[10]中激光能量密度随电流变化衰减率的数据, 通过插值处理后得到当激光与等离子弧热源 ($I=50\text{ A}$) 间距为0时 α 为25%。根据等离子弧热流密度在空间上近似符合高斯分布, α 与电弧的 N_e, N_i, T 之间存在函数关系以及文献[10]的结果, 可合理地假定 α 在空间上也符合高斯分布。

$$\alpha = \alpha_0 \exp\left(\frac{-3d^2}{R_{\text{arc}}^2}\right), \quad (3)$$

式中: α_0 为热源间距 $d=0$ 时的吸收系数。

1.3 边界条件

焊接工件与周围环境之间, 存在对流和辐射两种热传导方式, 为了简化处理, 将两种热传导方式的作用综合考虑, h_c 代表辐射换热系数与对流换热系数合成的综合换热系数, 表示为^[11]

$$h_c = 2.41 \times 10^{-3} \epsilon T_s^{1.61}, \quad (4)$$

式中: ϵ 是工件表面的辐射率, 取为0.4; T_s 为焊接工件表面的温度。

1.4 材料的热物理性能参数处理方法

为了间接地考虑熔池流动对焊接热传导过程的影响, 采用了热传导率随温度升高而上升的方法^[12, 13], 并借鉴了文献[12]的热传导率数据。焊接工件被加热部位的温度超过熔点后会发生固液相变, 可采用热焓法处理, 焓值定义为^[14]

$$H = h + \Delta H, \quad (5)$$

$$\Delta H = \beta L, \quad \beta = \frac{T - T_m}{T_1 - T_m}, \quad T \in [T_m, T_1], \quad (6)$$

式中: H 为热焓值; β 为液相分数值; L 为熔化潜热值; T_m 为固化温度; T_1 为液化温度。不随温度变化的1420铝锂合金热物理特性参数见表1^[15]。

表1 1420铝锂合金的热物理特性参数

固化温度 $T_m / ^\circ\text{C}$	液化温度 $T_l / ^\circ\text{C}$	密度 $\rho / (\text{kg} \cdot \text{m}^{-3})$	熔化潜热 $L / (\text{J} \cdot \text{kg}^{-1})$	比热容 $c_p / (\text{J} \cdot \text{kg}^{-1} \cdot ^\circ\text{C}^{-1})$
560	650	2 500	3.91×10^5	1 203

2 有限元分析模型

所分析的复合焊过程采用电弧在前, 激光在后的旁轴复合方式, 热源间距 d 可调整, 焊接对象为2 mm厚1420铝锂合金薄板, 其中 $P_{\text{laser}} = 2.8\text{ kW}$, $I = 50\text{ A}$, $U = 15\text{ V}$, $v = 3.6\text{ m/min}$ 。试验测试后确定 $R_{\text{laser}} = 0.3\text{ mm}$, $R_{\text{arc}} = 1.5\text{ mm}$ 。由于工件关于焊缝中心线对称, 只对其一半进行建模即可, 计算网格使用18 800个Solid70单元, 21 890个节点, 尺寸为 $24\text{ mm} \times 9.6\text{ mm} \times 2\text{ mm}$ (图2)。焊缝处的温度梯度变化较大, 为保证计算精度, 该处单元较密, 最小单元为 $0.15\text{ mm} \times 0.15\text{ mm} \times 0.2\text{ mm}$ 。计算模型是在ANSYS平台上实现的。设工件的初始温度为 $20\text{ }^\circ\text{C}$, 总计算时间为0.3125 s, 步长为0.0125 s。

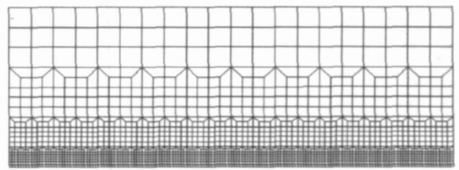


图2 计算网格

Fig. 2 Mesh of computation

3 计算结果与讨论

3.1 不同热源间距条件下的热循环

根据所建立的复合热源模型, 对四个热源间距条件下 ($d=0, 1, 2, 4\text{ mm}$) 的温度场进行了计算, 得到了焊缝中心线在 $y=8.25\text{ mm}, z=0, 1, 2\text{ mm}$ 处3点的热循环曲线(图3)。

由计算结果可知, 在工件的中心焊缝处, 随着热

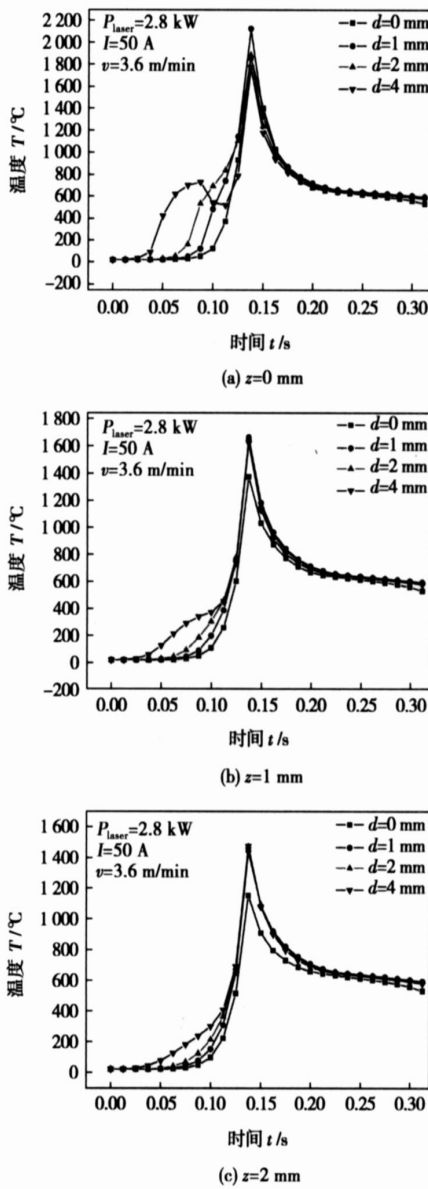


图 3 不同热源间距条件下的热循环曲线

Fig. 3 Thermal cycle of workpiece in different distances of two heat sources

源间距的增加, 等离子弧热源对工件的预热作用愈强。电弧在前、激光在后的复合焊接方式会使焊接部位处于高温状态的时间延长, 有利于提高工件对激光的吸收率。不同的热源间距对于复合焊接过程中的冷却过程基本没有影响, 不管那一种热源间距情况下, 均保持快速凝固的特点。

3.2 不同热源间距条件下的熔池形状

根据不同热源间距时温度场的计算结果, 以铝锂合金的液化温度 $650 \text{ }^\circ\text{C}$ 为温度场中等温线的最大值, 此等温线可以认为是熔池固液面的分界线, 即此分界线所包围的区域为熔池。如图 4, 图 5 所示, 随着热源间距的加大, 激光和等离子弧的熔池显示出

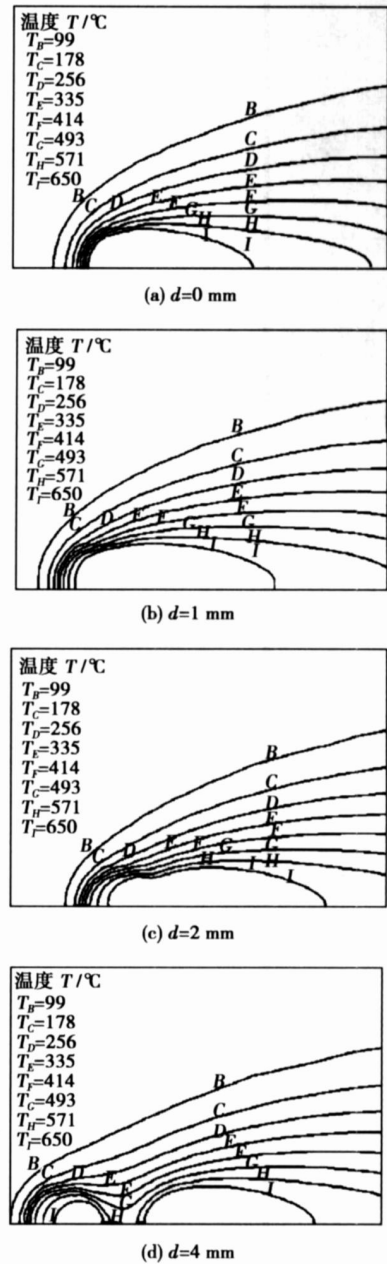


图 4 不同热源间距条件下的工件正面温度场

Fig. 4 Temperature distribution of front of workpiece in different distances of two heat sources

从熔合到逐渐分离的过程。当 $d < 3 \text{ mm}$ 时, 激光与等离子弧同时作用在同一个熔池中, 此时等离子弧除了预热作用, 两个热源在熔池中也有相互作用, 关于此作用将在今后的论文中阐述。当 $d = 4 \text{ mm}$ 时, 二者的熔池已经分离, 如图 4d, 图 5d 所示, 故当 $d > 4 \text{ mm}$ 时等离子弧对工件主要起到预热作用。随着热源间距的变化, 熔池在焊缝中心方向的长度在不断变化, 当热源间距为 2 mm 时形成的熔池长度最大。通过图 5d 可知, 等离子弧所产生的熔深很浅, 故激光热源在复合热源总的能量配比中所占比重

大, 激光热源能量对焊缝成形起主要作用。

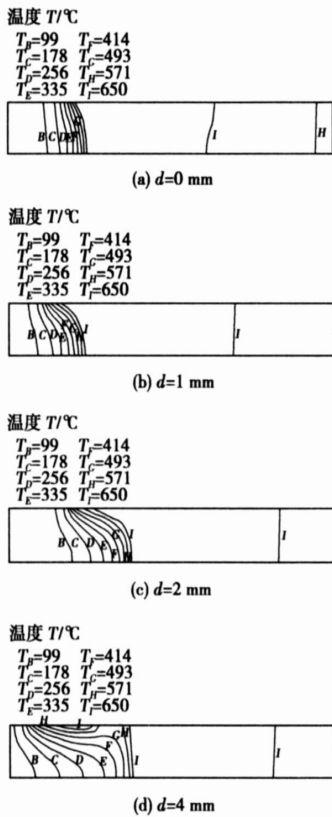


图 5 不同热源间距条件下的焊缝中心温度场

Fig. 5 Temperature distribution of weld centre in different distances of two heat sources

3.3 计算结果的验证

采用与计算过程相同的工艺参数进行了 2 mm 厚 1420 铝锂合金板焊接试验, 复合方式和工艺参数如第 2 节所述, 然后测量了工件正、背面的熔宽, 结果如图 6 所示。

为了分析热源相互作用对焊缝正面、背面熔宽的影响, 针对不同热源间距的条件, 分别计算了未考虑热源相互作用(即将两个热源热量线性叠加)和考虑热源相互作用的焊缝正背面熔宽。通过图 6a 中模拟数据与试验数据的对比可知, 未考虑热源相互作用得到的熔宽变化规律与试验得到的规律在热源间距较小的情况下有差别, 前者是一个单调下降的过程, 而后者在 $d=1$ mm 处有一个尖峰, 故采用两个热源线性叠加得到的计算结果是不符合实际的。在复合焊温度场数值模拟中应该考虑热源的相互作用。图 6b 表明焊接试验所得到的熔宽变化规律与模拟计算所得规律符合较好, 二者均反映了热源间距为 0 并不导致正面熔宽最大, 而当 $d=1$ mm 时

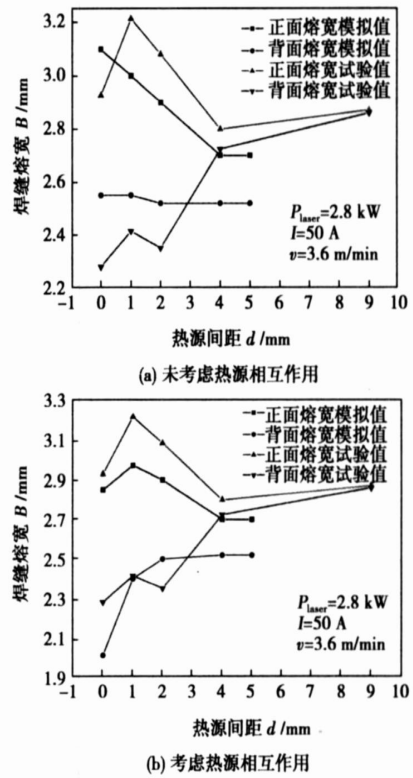


图 6 计算与试验结果对比

Fig. 6 Comparison of simulation and experiment results

正面熔宽最大。对于焊缝背面的熔宽, 二者的趋势相同, 但是在 $d=2$ mm 处, 计算结果大于试验结果, 分析认为是由于误差造成的, 故所提出的考虑热源相互作用的模型符合客观实际。

在图 6 中, 当热源间距为 9 mm 时, 正、背面熔宽的试验值有小幅度地增加, 这可能是由于随着热源间距的增加, 等离子弧与工件的夹角更接近垂直, 故等离子弧对工件加热的效率提高, 导致工件表面对激光的吸收系数上升所致, 所提出的模型中并没有考虑等离子弧与工件之间的夹角对焊接过程的影响, 故计算结果没有反映此变化。

4 结 论

(1) 建立了激光—等离子弧复合焊三维热源模型, 考虑了激光与等离子弧在不同热源间距条件下的相互作用。

(2) 随着热源间距的加大, 激光熔池与等离子弧熔池由熔合变为分离, 根据假设条件, 模拟计算结果表明当热源间距为 4 mm 时二者已经分离, 此时等离子弧热源对工件主要起到预热作用。

(3) 利用所建立的模型, 预测了不同热源间距

条件下激光—等离子弧复合焊缝的熔宽,且与试验得到的规律趋势相同,误差在10%以内,而采用不对热源相互作用修正的模型,计算结果与试验结果之间存在明显差异,因此复合焊热源模型需考虑热源的相互作用。

(4) 通过模拟计算发现,激光与等离子弧的热源间距对焊缝成形有影响,热源间距为0时并不能得到最大的熔宽,试验也证实了这一结果。

参考文献:

- [1] Claus Bagger, Flemming O Olsen. Review of laser hybrid welding [J]. *Journal of Laser Application*, 2005, 17(1), 2—14.
- [2] Blundell N, Biffin J, Johnson T, *et al.* High speed, augmented laser welding of thin sheet metals[C] // 5th International Conference on Trends in Welding Research, ASM International, 1998: 483—487.
- [3] Muneharu Kutsuna, Liang Chen. Interaction of both plasmas in CO₂ laser-MAG hybrid welding of carbon steel[C] // First International Symposium on High-Power Laser Macroprocessing, SPIE V4831, 2003: 341—346.
- [4] Zhou J, Zhang W H, Tsai H L, *et al.* Modeling the transport phenomena during hybrid laser-MIG welding process [J]. *American Society of Mechanical Engineers, Heat Transfer Division*, 2003, 374(3): 161—168.
- [5] Chen Yanbin, Li Liqun, Fang Junfei, *et al.* Temperature field simulation of laser-TIG hybrid welding [J]. *China Welding*, 2003, 12(1): 62—66.
- [6] 刘黎明,迟鸣声,宋刚,等. 镁合金激光—TIG复合热源焊接热源模型建立及其数值模拟[J]. *机械工程学报*, 2006, 42(2): 82—85.
- [7] Bin Hu. Nd/YAG laser-assisted arc welding [D]. Holland: Delft University of Technology, 2002.
- [8] 史耀武. 材料焊接工程(上)[M]. 北京: 化学工业出版社, 2006.
- [9] Semak V V, Steele R J, Fuerschbach P W, *et al.* Role of beam absorption in plasma during laser welding [J]. *Journal of Physics D: Applied Physics* 2000, 33(10): 1179—1185.
- [10] 陈彦宾. 激光—TIG复合焊接物理特性研究[D]. 哈尔滨: 哈尔滨工业大学, 2003.
- [11] Goldak J, Bibby M, Moore J, *et al.* Computer modeling of heat flow in welds [J]. *Metallurgical and Materials Transactions B: Process Metallurgy and Materials Processing Science*, 1986, 17B: 587—600.
- [12] 吴会强,冯吉才,何景山,等. 电子束焊接过程温度场应力场三维有限元仿真[J]. *焊接技术*, 2004, 33(6): 10—12.
- [13] 魏艳红,刘仁培,董祖珏. 不锈钢焊接凝固裂纹温度场的数值模拟[J]. *焊接学报*, 1999, 20(3): 199—204.
- [14] Voller V R, Swaminathan C R. Generalized source-based method for solidification phase change [J]. *Numerical Heat Transfer, Part B*, 1991, 19(2): 175—189.
- [15] 王祝堂,田荣璋. 铝合金及其加工手册(第二版)[M]. 长沙: 中南大学出版社, 2000.

作者简介: 李志宁,男,1972年出生,博士研究生,讲师。主要研究方向为高能束加工过程控制。发表论文16篇。

Email: lizn03@mails.tsinghua.edu.cn

vector; seam tracking; welding mobile robot

Simulation on equivalent stress in soldered joints of QFP devices with different leads XUE Songbai, WU Yuxiu, HAN Zongjie, HUANG Xiang (College of Materials Science and Technology, Nanjing University of Aeronautics and Astronautics, Nanjing 210016, China). p17–20

Abstract: Finite element method was used to simulate residual stress in soldered joints of QFP devices with different leads. Results indicate that the PCB is warped outward but the distortion is small. The ceramic plate is warped upward and the distortion of its integral structure is obvious after thermal cycle. At the same time, the expanding of the crack in soldered joint will be aggravated for the pull stress from ceramic plate to the lead.

The largest strain value emerges in outside of the soldered joints. The equivalent stress is relatively large in the root and toe of the soldered joint of QFP gull wing lead that the stress is larger in the root than that in the toe but that in the middle area of the soldered joint is the least. The simulating results show that the largest stress was endured by the soldered joint of QFP with 32 leads, larger stress endured by the soldered joint of QFP with 48 leads, and the least stress endured by the QFP with 100 leads. The tensile test shows that the soldered joint of the QFP device with 100 leads possesses the biggest tensile strength than that of the QFP with 48 leads and the QFP with 32 leads, which is concordant with the numerical simulation results.

Key words: finite element method; equivalent stress; life prediction; quad flat package

A zero-voltage and zero-current welding inverter with current doubler rectifier CHEN Yarming¹, WU Huifang¹, CAO Biao², WANG Zhiqiang² (1. College of Electrical Engineering, Guangxi University, Nanning 530004, China; 2. Electric Power College, South China University of Technology, Guangzhou 510641, China). p21–24

Abstract: A full-bridge with zero-voltage and zero-current switching (ZVZCS) PWM DC-DC welding inverter by employing phase-shift and current-doubler-rectifier is presented. The zero-voltage turn-on was achieved for the leading-leg of the converter, and zero-current turn-off was achieved for the lagging-leg, and the rectifier diodes in the secondary side were turned off naturally. All the power semiconductors in the converter were operated with soft-switching condition. Hence the switching stresses, losses and interferences were reduced, and electromagnetic compatibility is improved. It is especially suitable for the high power output applications. The switching frequency can be increased, and the dynamic response can be improved. The soft-switching operating range and the design considerations were discussed. Finally, a 2 kW welding inverter was designed, and the experimental results show its good performances.

Key words: welding inverter; phase-shift control; zero-voltage-switch; zero-current-switch; current-doubler rectifier

Modeling and simulation of weaving arc in submerged arc welding HONG Bo, HUANG Jun, PAN Jiluan, QU Yuebo* (Department of Mechanical Engineering, Xiangtan University, Xiangtan

411105, Hunan, China). p25–28

Abstract: According to the characteristics of submerged arc welding with alternative wire feed system, the seam tracking process of the submerged arc welding was studied. The models to simulate welding power, welding arc and scanning the V groove were founded, and the general simulation model of welding system was established based on these models. The influences of groove type, welding power and forms of metal transfer on the output welding current were studied and the effects of the main parameters of arc sensor on seam deviation and welding parameters were also analyzed. The studies offer a theoretical foundation to the establish the auto seam tracking system of weaving arc sensor in submerged arc welding.

Key words: weaving arc; seam tracking; modeling; simulation

Numerical simulation on temperature field in laser-plasma arc hybrid welding LI Zhining, CHANG Baohua, DU Dong, WANG Li (Key Laboratory for Advanced Materials Processing Technology, Tsinghua University, Beijing 100084, China). p29–33

Abstract: A three dimensional heat transfer model was put forward for the laser-plasma arc hybrid welding, which combines the mathematical models of two heat sources. The model of laser welding is Gaussian volume heat source and its peak heat flux decreases with depth, and the model of plasma arc is Gaussian plane heat source. The influence, induced by reaction between laser beam and plasma arc, was mainly studied in the model. Based on the model, the temperature distribution of 2 mm 1420 Al-Li alloy plate was obtained by FEM computation for laser-plasma arc hybrid welding in different distances of two heat sources. The hybrid welding experiments were conducted and show that the simulation results are well agreed with the experimental results. The result proves that the heat transfer model is more close to physical reality. This paper is instructive to research on heat transfer and process about laser-plasma arc hybrid welding.

Key words: laser-plasma arc hybrid welding; finite element method; numerical simulation; Al-Li alloy

Chromium Carbide in situ synthesis by vacuum electron beam

LU Fenggui, LU Binferg, TANG Xinghua, YAO Shun (Welding Engineering Institute, Shanghai Jiaotong University, Shanghai 200030, China). p34–36

Abstract: High hardness composite chromium carbide was successfully produced by in situ synthesis technology, which make it possible to prepare high temperature wear resistance alloy. Chemical reaction among Cr, Fe and C powder which were mixed and laid on the metal surface occurred through vacuum electron beam rotary scanning heating. The resultant of reaction at the metal was identified as Cr₇C₃ composite by X-ray diffraction. And microstructure of composite shows that there is chromium carbide congregated at the metal surface. The mechanical properties show that surface hardness is higher than that of base metal because of chromium carbide. In situ synthesis technology was proved to be a good way to realize metal surface modification.

Key words: vacuum electron beam; in situ synthesis; chromium carbide